

CERN-PH-EP-2014-092
14 May 2014

Suppression of $\psi(2S)$ production in p-Pb collisions at $\sqrt{s_{NN}} = 5.02$ TeV

ALICE Collaboration

Abstract

The ALICE Collaboration has studied the inclusive production of the charmonium state $\psi(2S)$ in proton-lead (p-Pb) collisions at the nucleon-nucleon centre of mass energy $\sqrt{s_{NN}} = 5.02$ TeV at the CERN LHC. The measurement was performed at forward ($2.03 < y_{cms} < 3.53$) and backward ($-4.46 < y_{cms} < -2.96$) centre of mass rapidities, studying the decays into muon pairs. In this paper, we present the inclusive production cross sections $\sigma_{\psi(2S)}$, both integrated and as a function of the transverse momentum p_T , for the two y_{cms} domains. The results are compared to those obtained for the 1S vector state (J/ψ), by showing the ratios between the production cross sections, as well as the double ratios $[\sigma_{\psi(2S)}/\sigma_{J/\psi}]_{pPb}/[\sigma_{\psi(2S)}/\sigma_{J/\psi}]_{pp}$ between p-Pb and proton-proton collisions. Finally, the nuclear modification factor for inclusive $\psi(2S)$ is evaluated and compared to the measurement of the same quantity for J/ψ and to theoretical models including parton shadowing and coherent energy loss mechanisms. The results show a significantly larger suppression of the $\psi(2S)$ compared to that measured for J/ψ and to models. These observations represent a clear indication for sizeable final state effects on $\psi(2S)$ production.

arXiv:1405.3796v3 [nucl-ex] 12 Oct 2015

The physics of charmonia, bound states of the charm (c) and anti-charm (\bar{c}) quarks, is an extremely broad and interesting field of investigation [1]. The description of the various states and the calculation of their production cross sections in hadronic collisions involve an interplay of perturbative and non-perturbative aspects of Quantum ChromoDynamics (QCD) [2], which still today represent a significant challenge for theory [3]. Charmonium states can have smaller sizes than light hadrons (down to a few tenths of a fm) and large binding energies (> 500 MeV) [4]. These properties make charmonia a useful probe of the hot nuclear matter created in ultrarelativistic heavy-ion collisions, which can be seen as a plasma of deconfined quarks and gluons (QGP) (see [5] for a recent overview of QGP studies). In particular, the $c\bar{c}$ binding can be screened by the high density of colour charges present in the QGP, leading to a suppression of the yields of charmonia in high-energy nuclear collisions compared to the corresponding production rates in elementary pp collisions at the same energy [6]. In the so-called “sequential suppression” scenario, the melting of a bound $c\bar{c}$ state occurs when the temperature of the hot medium exceeds a threshold dissociation temperature [7, 8], which depends on the binding energy of the state and can be calculated in lattice QCD [9]. At LHC energies, where the number of produced $c\bar{c}$ pairs is large, this suppression effect can be partly counterbalanced by charmonium “regeneration” processes due to the recombination of charm quarks that occurs as the system cools and hadrons form [10–12].

Among the charmonium states, the strongly bound S-wave J/ψ and the weakly bound radially excited $\psi(2S)$ have received most attention in the context of QGP studies. Both decay to lepton pairs with a non-negligible branching ratio (5.93% and 0.77%, respectively, for the $\mu^+\mu^-$ channel [13]). The results obtained by the NA50 collaboration at the CERN SPS showed a significant suppression of the J/ψ production in Pb-Pb collisions at $\sqrt{s_{NN}} = 17$ GeV [14] and a comparatively larger suppression of the $\psi(2S)$ [15], in qualitative agreement with sequential suppression models. However, the same experiment also detected a significant suppression of both states (although not as strong as in Pb-Pb) in proton-nucleus (p-A) collisions [16], where no QGP formation was expected. The same observation was made by other fixed-target experiments studying p-A collisions at Fermilab (E866 [17]) and HERA (HERA-B [18]). It was indeed realized that the charmonium yields are also sensitive to the presence of cold nuclear matter (CNM) in the target nucleus, and various mechanisms (nuclear parton shadowing [19], $c\bar{c}$ break-up via interaction with nucleons [20–22], initial/final state energy loss [23]) were taken into account in order to describe experimental observations. In particular, these experiments observed a stronger suppression for $\psi(2S)$ relative to J/ψ at central rapidity, while at forward rapidity no difference was found within uncertainties. This feature of the results was interpreted in terms of pair break-up: at central rapidity the time spent by the $c\bar{c}$ state in the nuclear medium (crossing time) is typically larger than the formation time of the resonances (~ 0.1 fm/c [24, 25]), so that the loosely bound $\psi(2S)$ can be more easily dissociated than the J/ψ . Conversely, in forward production the crossing time is smaller than the formation time and the influence of the nucleus on the pre-hadronic state is the same, independent of the particular resonance being produced [26].

More generally, the study of charmonia in p-A collisions can be used as a tool for a quantitative investigation of the aforementioned processes, relevant in the context of studies of the strong interaction. Therefore, measurements at high energies are important to test our understanding of the various mechanisms. In particular, the pair break-up cross sections discussed above are expected to be strongly reduced due to the increasingly shorter time spent by the $c\bar{c}$ pair in CNM. On the other hand, the other effects listed above (shadowing, energy loss) are not expected to depend on the final quantum numbers of the charmonium states. In such a situation, a similar suppression for the two charmonium states should be observed in high-energy p-A collisions.

In the context of comparative studies between the resonances, the PHENIX experiment at RHIC has recently published results on the $\psi(2S)$ suppression at central rapidity for d-Au collisions at $\sqrt{s_{NN}} = 200$ GeV [27], by studying the nuclear modification factor $R_{dAu}^{\psi(2S)} = dN_{dAu}^{\psi(2S)}/dy / (N_{coll} \times dN_{pp}^{\psi(2S)}/dy)$, which corresponds to the ratio of the production yields in d-Au and pp at the same energy, normalized by the

number of nucleon-nucleon collisions in d-Au. The ratio of the nuclear modification factors $R_{\text{dAu}}^{\psi(2S)}/R_{\text{dAu}}^{J/\psi}$ is found to be smaller than 1, and strongly decreasing from peripheral to central d-Au events. The observation of a $\psi(2S)$ suppression stronger than that of the J/ψ is in contrast to the expectation of a similar suppression as described above. Data from the LHC can be useful to shed further light on this observation, as nuclear crossing times [25] may be as low as 10^{-4} fm/c for charmonium production at forward rapidity, implying a negligible influence of pair break-up processes and, in more general terms, to test our understanding of charmonium propagation in CNM.

In this Letter, we present the first measurement of inclusive $\psi(2S)$ production in $\sqrt{s_{\text{NN}}} = 5.02$ TeV p-Pb collisions at the LHC, carried out by the ALICE Collaboration, and we compare the results with those for J/ψ . The resonances were measured in the dimuon decay channel using the Muon Spectrometer (MS) [28], which covers the pseudorapidity range $-4 < \eta_{\text{lab}} < -2.5$. The other detectors involved in this analysis are: (i) the two innermost layers of the Inner Tracking System (Silicon Pixel Detectors, SPD), used for the determination of the primary vertex of the interaction and covering $|\eta_{\text{lab}}| < 2.0$ (first layer) and $|\eta_{\text{lab}}| < 1.4$ (second layer) [29]; (ii) the two VZERO scintillator hodoscopes, used mainly for triggering purposes and covering $-3.7 < \eta_{\text{lab}} < -1.7$ and $2.8 < \eta_{\text{lab}} < 5.1$ [30]; (iii) the Zero Degree Calorimeters (ZDC), at 112.5 m from the interaction point [31], used to remove collisions outside the nominal timing of the LHC bunches. Details of the ALICE experimental setup are provided elsewhere [32].

Due to the LHC design, the colliding beams have different energies per nucleon ($E_p = 4$ TeV, $E_{\text{Pb}} = 1.58 \cdot A_{\text{Pb}}$ TeV, where $A_{\text{Pb}} = 208$ is the mass number of the Pb nucleus). As a consequence, the centre of mass of the nucleon-nucleon collision is shifted by $\Delta y = 0.465$ with respect to the laboratory frame in the direction of the proton beam. Data were taken in two configurations, by inverting the sense of the orbits of the two beams. In this way, both forward ($2.03 < y_{\text{cms}} < 3.53$) and backward ($-4.46 < y_{\text{cms}} < -2.96$) centre of mass rapidities were covered, with the positive rapidity defined by the direction of the proton beam. We refer to the two data samples as p-Pb and Pb-p respectively. The integrated luminosities for the two data samples are $L_{\text{int}}^{\text{pPb}} = 5.01 \pm 0.19 \text{ nb}^{-1}$ and $L_{\text{int}}^{\text{PbP}} = 5.81 \pm 0.20 \text{ nb}^{-1}$ [33].

Data were collected with a dimuon trigger, defined as the coincidence of the minimum-bias (MB) condition with the detection of two opposite-sign muon candidates in the trigger system of the MS. The MB condition is a coincidence between signals in the two VZERO hodoscopes and has $> 99\%$ efficiency for non-single diffractive events [34]. For the muon candidates, a transverse momentum $p_{\text{T},\mu} = 0.5$ GeV/c trigger threshold is applied. The effect of this threshold is not sharp, and the single muon trigger efficiency reaches its plateau value ($\sim 96\%$) for $p_{\text{T},\mu} \sim 1.5$ GeV/c. The offline event selection, the muon reconstruction and identification criteria and the kinematic cuts applied at the single and dimuon levels are identical to those described in [35]. In addition, a cut on the transverse distance from the primary vertex of each of the reconstructed muon tracks, weighted with its momentum ($p\text{DCA}$), was performed. Tracks with $p\text{DCA} > 6 \times \sigma_{p\text{DCA}}$ were rejected. The quantity $\sigma_{p\text{DCA}}$ is the $p\text{DCA}$ resolution, which is obtained from data, taking into account the resolution on track momentum and slope [36]. Such a track cut reduces the background continuum by a few percent without affecting the resonances.

The extraction of the resonance signals is carried out by means of a fit to the dimuon invariant mass spectrum, as illustrated in Fig. 1 for the two rapidity ranges under study. The J/ψ and $\psi(2S)$ line shapes are described either by Crystal Ball (CB) functions [37], with asymmetric tails on both sides of the peak, or by pseudo-Gaussian functions [38]. The parameters of the resonance shapes are obtained by means of a Monte-Carlo (MC) simulation. Pure J/ψ and $\psi(2S)$ signal samples are generated, and then tracked and reconstructed in the experimental setup with the same procedure applied to real data. The choice of the MC kinematic distributions of charmonia is discussed below when introducing the acceptance calculation. Due to the large signal to background ratio (S/B) in the J/ψ mass region and in order to account for small deviations of the mass ($\sim 0.1\%$) and width ($\sim 10\%$) between MC and data, the corresponding parameters are left free in the fit. For the $\psi(2S)$, due to the less favourable S/B,

the mass and widths are constrained by those for the J/ψ using the following relations, which involve the corresponding MC quantities: $m_{\psi(2S)} = m_{J/\psi} + (m_{\psi(2S)}^{MC} - m_{J/\psi}^{MC})$ and $\sigma_{\psi(2S)} = \sigma_{J/\psi} \cdot (\sigma_{\psi(2S)}^{MC} / \sigma_{J/\psi}^{MC})$. Alternative values of the $\psi(2S)$ mass resolution have also been tested, allowing the ratio $(\sigma_{\psi(2S)}^{MC} / \sigma_{J/\psi}^{MC})$ to vary within 10% [36]. Finally, the parameters of the asymmetric tails, which can hardly be constrained by the data, are kept fixed to their MC values. Additional sets of tails, obtained from the MC, but sampling the y_{cms} and p_T phase space, have also been tested. The dependence of the extracted J/ψ and $\psi(2S)$ yields on the variation of the tails and on the $\psi(2S)$ mass resolution is included in the systematic uncertainty on the signal extraction. The background continuum under the resonances is parameterized by empirical shapes, using a polynomial times an exponential function or a Gaussian having a width increasing with mass. In order to assess the systematic uncertainty on signal extraction, fits with various combinations of the signal and background shapes are performed, and the start/end point of the fit range is also varied. The raw $\psi(2S)$ yields and their statistical uncertainty is finally obtained as the average of the results of the various fits performed, while the systematic uncertainty is calculated as the root-mean-square (RMS) of their distribution. This results in $N_{pPb}^{\psi(2S)} = 1069 \pm 130 \pm 102$ and $N_{PbPb}^{\psi(2S)} = 697 \pm 111 \pm 65$, where the first uncertainty is statistical and the second is systematic. The $\psi(2S)$ mass resolution extracted from the fits is ~ 70 MeV/ c^2 . As a cross-check, an alternative approach for signal extraction, based on event counting, was also tested. More precisely, after fitting the invariant mass distribution and subtracting the background contribution, the number of $\psi(2S)$ was obtained by integrating the background subtracted spectrum in the region $3.5 < m_{\mu\mu} < 3.8$ GeV/ c^2 . Corrections, based on the signal fitting functions, were applied to the measured number of counts to account for the fraction of $\psi(2S)$ outside of the integration region ($\sim 15\%$) and for the number of J/ψ falling inside the $\psi(2S)$ mass range ($\sim 8\%$). The results were found to be stable within 1% with respect to 0.1 GeV/ c^2 variations of the integration region. The number of J/ψ and $\psi(2S)$ extracted in this way are also in excellent agreement (i.e., well within the systematic uncertainties) with respect to the $N_{pPb}^{\psi(2S)}$ and $N_{PbPb}^{\psi(2S)}$ values quoted above.

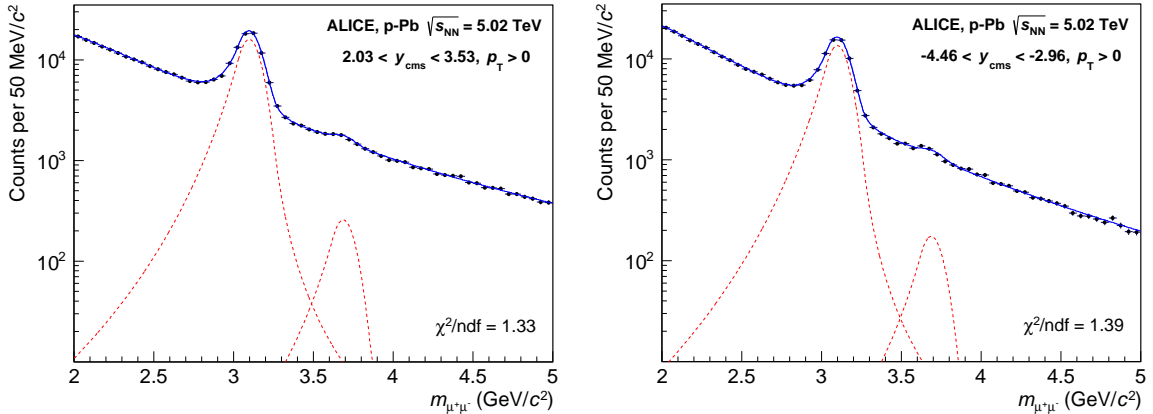


Fig. 1: Opposite-sign dimuon invariant mass spectra for the p-Pb (left) and Pb-p (right) data samples, together with the result of a fit. For the fits shown here, Crystal Ball functions (shown as dashed lines) and a variable-width Gaussian have been used for the resonances and the background, respectively. The χ^2/ndf refers to the goodness of the signal and background combined fit in the displayed mass range.

The acceptance times efficiency values ($A \times \varepsilon$) for the $\psi(2S)$ were evaluated using MC simulations in a similar way as detailed in [35] for the J/ψ . The input p_T distributions were obtained from those used for the J/ψ [35], scaled such that $\langle p_T \rangle_{pPb, 5.02\text{TeV}}^{\psi(2S)} = \langle p_T \rangle_{pPb, 5.02\text{TeV}}^{J/\psi} \times (\langle p_T \rangle_{pp, 7\text{TeV}}^{\psi(2S)} / \langle p_T \rangle_{pp, 7\text{TeV}}^{J/\psi})$, and using the $\sqrt{s} = 7$ TeV pp values from LHCb [39, 40] obtained in the slightly larger range $2 < y_{cms} < 4.5$. The input y distributions were obtained from those used for the J/ψ assuming a scaling of the widths with $y_{max}^{\psi(2S)} / y_{max}^{J/\psi}$, where $y_{max}^i = \log(\sqrt{s}/m_i)$ is the maximum rapidity for the resonance i at the \sqrt{s} value under study. An unpolarized distribution for the $\psi(2S)$ was assumed, according to the results obtained in pp collisions at $\sqrt{s} = 7$ TeV by the CMS and LHCb experiments [41, 42]. The systematic uncertainty for

the $\psi(2S)$ acceptance was calculated as the maximum spread of the values obtained by assuming as alternative input distributions those used for the J/ψ itself and amounts to 1.8% (2.5%) for p-Pb (Pb-p).

The efficiency of the tracking and trigger detectors of the MS was taken into account in the MC simulations by means of a map of dead channels (tracking) and by building efficiency tables for the detector elements (trigger). The evolution of the detector performance throughout the data taking was followed in the MC, by generating a number of events which is proportional to the run-by-run number of dimuon triggers, in order to properly weight the detector conditions over the entire data taking. The systematic uncertainties on the efficiencies were obtained with algorithms based on real data, with the same procedure adopted in [35], and they are identical for J/ψ and $\psi(2S)$. A small uncertainty related to the efficiency of the matching between tracking and triggering information was also included [35].

The p_T -integrated $A \times \varepsilon$ values for $\psi(2S)$ production, obtained with this procedure, are 0.270 ± 0.014 (p-Pb) and 0.184 ± 0.013 (Pb-p), where the lower value for Pb-p is mainly due to a smaller detector efficiency in the corresponding data taking period, related to a worse detector performance. The quoted uncertainties are systematic and are obtained as the quadratic sum of the uncertainties on MC input, tracking, triggering and matching efficiencies. The statistical uncertainties are negligible.

The cross section times the branching ratio $\text{B.R.}(\psi(2S) \rightarrow \mu\mu)$ for inclusive $\psi(2S)$ production in p-Pb collisions (and similarly for Pb-p) is:

$$\text{B.R.}_{\psi(2S) \rightarrow \mu^+\mu^-} \cdot \sigma_{\text{pPb}}^{\psi(2S)} = \frac{N_{\psi(2S) \rightarrow \mu\mu}^{\text{cor}}}{L_{\text{int}}^{\text{pPb}}} \quad (1)$$

where $N_{\psi(2S) \rightarrow \mu\mu}^{\text{cor}}$ is the number of $\psi(2S)$ corrected for $A \times \varepsilon$, and $L_{\text{int}}^{\text{pPb}}$ is the integrated luminosity, calculated as $N_{\text{MB}}/\sigma_{\text{pPb}}^{\text{MB}}$. N_{MB} is the number of MB events, obtained as the number of dimuon triggers divided by the probability of having a triggered dimuon in a MB event. The N_{MB} numerical values and uncertainties are the same as those quoted in [35]. The cross sections for the occurrence of the MB condition, $\sigma_{\text{pPb}}^{\text{MB}}$, are measured in a vdM scan [33] to be 2.09 ± 0.07 b for the p-Pb configuration and 2.12 ± 0.07 b for the Pb-p one. The luminosity is also independently determined by means of a second luminosity signal, as described in [33]. The two measurements differ by at most 1% throughout the whole data-taking period and such a value is quadratically added to the luminosity uncertainty. The $\psi(2S)$ cross section values are:

$$\begin{aligned} \text{B.R.} \cdot \sigma_{\text{pPb}}^{\psi(2S)}(2.03 < y_{\text{cms}} < 3.53) &= 0.791 \pm 0.096(\text{stat.}) \pm 0.091(\text{syst.uncorr.}) \pm 0.013(\text{syst.corr.}) \mu\text{b} \\ \text{B.R.} \cdot \sigma_{\text{Pbp}}^{\psi(2S)}(-4.46 < y_{\text{cms}} < -2.96) &= 0.653 \pm 0.104(\text{stat.}) \pm 0.080(\text{syst.uncorr.}) \pm 0.010(\text{syst.corr.}) \mu\text{b} \end{aligned}$$

The systematic uncertainties for the $\psi(2S)$ cross section measurement are obtained as the quadratic sum of the various contributions listed in Table 1. The splitting between uncorrelated and correlated sources is also summarized there. The corresponding values for the J/ψ can be found in [35].

The study of the cross section ratio between $\psi(2S)$ and J/ψ , and the comparison of this ratio between different systems, offers a powerful tool to investigate nuclear effects on charmonium production. In addition, several systematic uncertainties cancel, or are significantly reduced, when studying such ratios. In particular, in the present analysis, the tracking, trigger and matching efficiencies, as well as the normalization-related quantities, cancel out. For the MC input, the fraction of the uncertainty related to the choice of the J/ψ kinematical distribution [35] cancels in the cross section ratios, and the remaining 1% (2%) uncertainty for p-Pb (Pb-p) is assigned to this source. Finally, the uncertainty on signal extraction is considered as uncorrelated between J/ψ and $\psi(2S)$, and its value for the cross section ratios amounts to 10% for both p-Pb and Pb-p. The resulting values are:

	B.R. $\cdot \sigma_{pPb}^{\psi(2S)}$	B.R. $\cdot \sigma_{PbP}^{\psi(2S)}$
Tracking efficiency	4	6
Trigger efficiency	2.8 (2 – 3.5)	3.2 (2 – 3.5)
Signal extraction	9.5 (8 – 11.9)	9.3 (8.6 – 12.7)
MC input	1.8 (1.5 – 1.5)	2.5 (1.5 – 1.7)
Matching efficiency	1	1
$L_{\text{int}}(\text{uncorr.})$	3.4	3.1
$L_{\text{int}}(\text{corr.})$	1.6	1.6

Table 1: Systematic uncertainties (in percent) affecting the measurement of inclusive $\psi(2S)$ cross sections. The L_{int} uncertainties are splitted in two components, respectively uncorrelated and correlated between p-Pb and Pb-p, as detailed in [33]. All the other uncertainties are uncorrelated between forward and backward rapidity. Uncertainties refer to p_T -integrated quantities and, where they depend on p_T , the corresponding maximum and minimum values are also quoted. The efficiency-related uncertainties refer to muon pairs.

$$\frac{\text{B.R.}_{\psi(2S) \rightarrow \mu^+ \mu^-} \cdot \sigma^{\psi(2S)}}{\text{B.R.}_{J/\psi \rightarrow \mu^+ \mu^-} \cdot \sigma^{J/\psi}} (2.03 < y_{\text{cms}} < 3.53) = 0.0154 \pm 0.0019(\text{stat.}) \pm 0.0015(\text{syst.})$$

$$\frac{\text{B.R.}_{\psi(2S) \rightarrow \mu^+ \mu^-} \cdot \sigma^{\psi(2S)}}{\text{B.R.}_{J/\psi \rightarrow \mu^+ \mu^-} \cdot \sigma^{J/\psi}} (-4.46 < y_{\text{cms}} < -2.96) = 0.0116 \pm 0.0018(\text{stat.}) \pm 0.0011(\text{syst.})$$

In Fig. 2 we compare these ratios with the corresponding ALICE results for pp collisions [36], obtained in slightly different centre of mass energy and rapidity regions, $\sqrt{s} = 7$ TeV, $2.5 < |y| < 4$, as no LHC pp results are available in the same kinematic conditions of proton-nucleus collisions. The pp ratios are significantly higher than those for p-Pb and Pb-p, which are compatible within uncertainties.

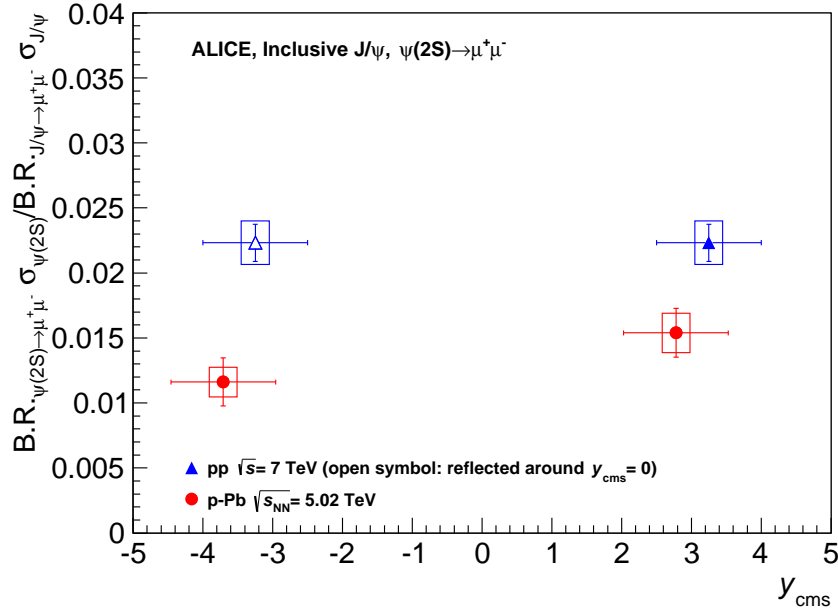


Fig. 2: The cross section ratios $\text{B.R.}_{\psi(2S) \rightarrow \mu^+ \mu^-} \cdot \sigma^{\psi(2S)} / \text{B.R.}_{J/\psi \rightarrow \mu^+ \mu^-} \cdot \sigma^{J/\psi}$ for p-Pb and Pb-p collisions, compared with the corresponding pp results at $\sqrt{s} = 7$ TeV [36]. The horizontal bars correspond to the width of the rapidity regions under study. The vertical error bars represent statistical uncertainties, the boxes correspond to systematic uncertainties.

The double ratio $[\sigma_{\psi(2S)} / \sigma_{J/\psi}]_{pPb} / [\sigma_{\psi(2S)} / \sigma_{J/\psi}]_{pp}$ is a useful quantity to directly compare the relative suppression of the two states between various experiments. For this analysis, since the collision energy

and the y -coverage of the p-Pb (Pb-p) and pp measurements are different, we have estimated the possible dependence of the $\sigma^{\psi(2S)}/\sigma^{J/\psi}$ vs \sqrt{s} and y in pp collisions. We start from the empirical observation that this ratio is very similar at collider energies over a rather broad range of y and \sqrt{s} . In particular, from the LHCb data ($\sqrt{s} = 7$ TeV, $2 < y < 4.5$) [39, 40] one gets 2.11% for the inclusive ratio integrated over p_T , while the corresponding value from CDF data ($p\bar{p}$ at $\sqrt{s} = 1.96$ TeV, $|y| < 0.6$) [43] is 2.05%, i.e., only 3% smaller (the latter quantity was obtained by extrapolating the CDF $\psi(2S)$ measurement to $p_T = 0$ with the phenomenological function $f(p_T) = (p_T)/[1 + (p_T/a)^2]^b$) [44]. The LHCb result can be extrapolated to central rapidity at $\sqrt{s} = 7$ TeV, assuming a Gaussian y -distribution for both resonances, with the width of the J/ψ distribution tuned directly on data [39] and that for $\psi(2S)$ obtained from the former assuming a scaling of the widths with $y_{\max}^{\psi(2S)}/y_{\max}^{J/\psi}$. The effect of this rescaling is small, leading to a 3% increase of the ratio. The central-rapidity ratio $\sigma_{\psi(2S)}/\sigma_{J/\psi}$ at $\sqrt{s} = 5.02$ TeV is then obtained by means of an interpolation between the CDF and LHCb-rescaled values, assuming a linear dependence of the ratio vs \sqrt{s} . Finally, one can extrapolate the ratio to the p-Pb and Pb-p rapidity ranges by using for the J/ψ the Gaussian shape obtained with the interpolation procedure described in [45] and for the $\psi(2S)$ the corresponding shape scaled with $y_{\max}^{\psi(2S)}/y_{\max}^{J/\psi}$. The difference between the measured value of $\sigma_{\psi(2S)}/\sigma_{J/\psi}$ for $\sqrt{s} = 7$ TeV, $2 < y_{\text{cms}} < 4.5$ and the results of the interpolation procedure to $\sqrt{s} = 5.02$ TeV, $2.03 < y_{\text{cms}} < 3.53$ ($-4.46 < y_{\text{cms}} < -2.96$) is -1.6% (-3.7%). When calculating the double ratio $[\sigma_{\psi(2S)}/\sigma_{J/\psi}]_{\text{pPb}}/[\sigma_{\psi(2S)}/\sigma_{J/\psi}]_{\text{pp}}$, we choose to use for pp the measured value at $\sqrt{s} = 7$ TeV, $2.5 < y_{\text{cms}} < 4$ [36] (rather than the interpolated one at $\sqrt{s} = 5.02$ TeV) and to include a 8% systematic uncertainty on this quantity, i.e., about twice the maximum difference between the measured values of the ratio in pp and the results of the interpolation procedure. A similar uncertainty would be obtained using as an input for the calculation, instead of the LHCb data, the more recent pp result from ALICE on $\sigma_{\psi(2S)}/\sigma_{J/\psi}$ [36].

The values of the double ratio are shown in Fig. 3, where they are also compared with the corresponding results obtained by the PHENIX experiment at $\sqrt{s_{NN}} = 200$ GeV, for $|y| < 0.35$ [27]. When forming the double ratio, the systematic uncertainties on the pp ratio, including the 8% contribution described in the previous paragraph, are considered as correlated between forward and backward rapidity, while the other systematic uncertainties are treated as uncorrelated. The dominating contributions to the systematic uncertainty come from the signal extraction and from the interpolation procedure used for the pp cross section. The ALICE results show that, compared to pp, the $\psi(2S)$ is more suppressed than the J/ψ to a 2.3σ (4.1σ) level in p-Pb (Pb-p). The PHENIX result shows a similar feature, at a 1.3σ level.

The suppression of charmonium states with respect to the corresponding pp yield can be quantified using the nuclear modification factor. For $\psi(2S)$, $R_{\text{pPb}}^{\psi(2S)}$ is obtained by combining $R_{\text{pPb}}^{J/\psi}$ [35] with the double ratio evaluated above:

$$R_{\text{pPb}}^{\psi(2S)} = R_{\text{pPb}}^{J/\psi} \cdot \frac{\sigma_{\text{pPb}}^{\psi(2S)}}{\sigma_{\text{pPb}}^{J/\psi}} \cdot \frac{\sigma_{\text{pp}}^{J/\psi}}{\sigma_{\text{pp}}^{\psi(2S)}} \quad (2)$$

In Fig. 4, $R_{\text{pPb}}^{\psi(2S)}$ is shown and compared with $R_{\text{pPb}}^{J/\psi}$. For the double ratios, the difference in the \sqrt{s} and y domains between p-Pb and pp is taken into account by the inclusion of the 8% systematic uncertainty described above. The other quoted uncertainties combine those from $R_{\text{pPb}}^{J/\psi}$ [35] with those for the double ratio, avoiding a double counting of the J/ψ related uncertainties. Figure 4 indicates that the $\psi(2S)$ suppression is much stronger than for the J/ψ and reaches a factor ~ 2 with respect to pp. The results are compared with theoretical calculations including either nuclear shadowing only [46] or coherent energy loss, with or without a shadowing contribution [47]. For the former mechanism, the values correspond to calculations performed for the J/ψ . However, due to the relatively similar kinematic distributions of gluons that produce the $c\bar{c}$ pair which will then hadronize to a J/ψ or a $\psi(2S)$, the shadowing effects

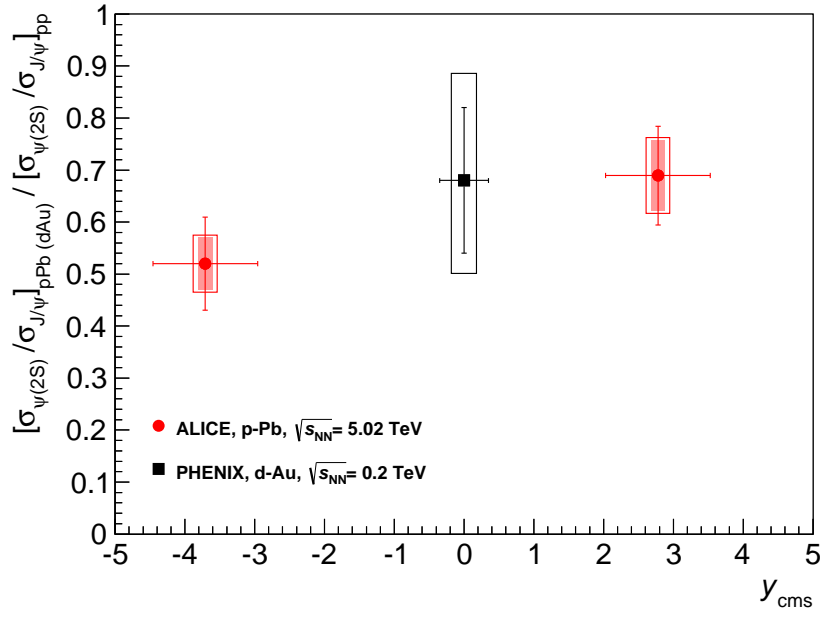


Fig. 3: Double ratios $[\sigma_{\psi(2S)}/\sigma_{J/\psi}]_{pPb} / [\sigma_{\psi(2S)}/\sigma_{J/\psi}]_{pp}$ for p-Pb and Pb-p collisions, compared to the corresponding PHENIX result at $\sqrt{s_{NN}} = 200$ GeV [27]. The horizontal bars correspond to the width of the rapidity regions under study. For ALICE, the vertical error bars correspond to statistical uncertainties, the boxes to uncorrelated systematic uncertainties, and the shaded areas to correlated uncertainties. For PHENIX, the various sources of systematic uncertainties were combined in quadrature.

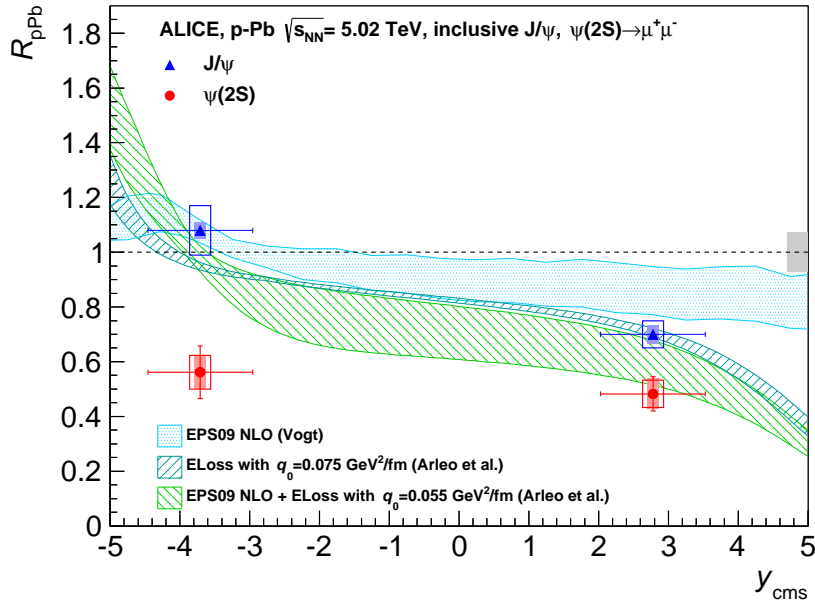


Fig. 4: The nuclear modification factor for $\psi(2S)$, compared to the corresponding quantity for J/ψ [35]. The horizontal bars correspond to the width of the rapidity regions under study. The vertical error bars correspond to statistical uncertainties, the boxes to uncorrelated systematic uncertainties, and the shaded areas to partially correlated uncertainties. The filled box on the right, centered on $R_{pPb} = 1$, shows uncertainties that are fully correlated between J/ψ and $\psi(2S)$. Model calculations tuned on J/ψ , and including nuclear shadowing [46] and coherent energy loss [47] are also shown. The corresponding calculations for $\psi(2S)$ produce identical values for the coherent energy loss mechanisms and a 2-3% larger result for nuclear shadowing and therefore are not shown.

are expected to be the same, within 2-3% [48], for the two charmonium states. No sensitivity to the final quantum numbers of the charmonium state is expected for coherent energy loss, implying that the calculations shown in Fig. 4 are valid for both resonances. As a consequence, all three models would predict an almost identical suppression for the $\psi(2S)$ and the J/ψ over the full rapidity range, with negligible theoretical uncertainties. This prediction is in strong disagreement with our data and clearly indicates that other mechanisms must be invoked in order to describe the $\psi(2S)$ suppression in proton-nucleus collisions.

The break-up cross section of the final state resonance due to interactions with CNM is expected to depend on the binding energy of the charmonium and such a mechanism would be a natural explanation for the larger suppression of $\psi(2S)$. However, this process becomes relevant only if the charmonium formation time τ_f is smaller than the time τ_c spent by the $c\bar{c}$ pair inside the nucleus. One can evaluate the average proper time τ_c spent in CNM as $\tau_c = \langle L \rangle / (\beta_z \gamma)$ [25], where $\langle L \rangle$ is the average length of nuclear matter crossed by the pair, which can be calculated in the framework of the Glauber model [49], $\beta_z = \tanh y_{c\bar{c}}^{\text{rest}}$ is the velocity of the $c\bar{c}$ along the beam direction in the nucleus rest frame, and $\gamma = E_{c\bar{c}}/m_{c\bar{c}}$. For $c\bar{c}$ pairs in the charmonium mass range emitted at $p_T = 0$ in the forward acceptance, one gets $\tau_c \sim 10^{-4}$ fm/c, while the corresponding value at backward rapidity is $\tau_c \sim 7 \cdot 10^{-2}$ fm/c. Estimates for the formation time τ_f range between 0.05 and 0.15 fm/c [24, 25]. In this situation, no break-up effects depending on the final charmonium state should be expected at forward rapidity, and even for backward production one has at most $\tau_f \sim \tau_c$ which would hardly accommodate the strong difference observed between $\psi(2S)$ and J/ψ suppression. As a consequence, other final state effects should be considered, including the interaction of the $c\bar{c}$ pair with the final state hadronic system created in the proton-nucleus collision.

The sizeable $\psi(2S)$ statistics collected in proton-nucleus collisions allows for a differential study of the various observables as a function of p_T , in the range $0 < p_T < 8$ GeV/c. We have chosen a transverse momentum binning which leads to similar relative statistical uncertainties in each bin over the p_T range covered. The analysis is carried out with the same procedure adopted for the integrated data samples. In particular, the systematic uncertainties are evaluated differentially in p_T , and their range is also reported in Table 1. In Fig. 5 the invariant mass spectra for the various p_T bins are shown, together with the result of the fits. In Fig. 6 the differential cross sections at forward and backward rapidity are presented. The systematic uncertainties on signal extraction, MC input and efficiencies are considered as bin-to-bin uncorrelated. The L_{int} uncertainties are correlated between the various p_T bins and partially correlated between p-Pb and Pb-p.

In Fig. 7 we present the p_T dependence of the double ratio $[\sigma_{\psi(2S)}/\sigma_{J/\psi}]_{\text{pPb}}/[\sigma_{\psi(2S)}/\sigma_{J/\psi}]_{\text{pp}}$, with the p-Pb J/ψ cross sections taken from [35] and the pp values from [36]. As for the integrated double ratio, the systematic uncertainties related to efficiencies and to normalizations cancel out for both proton-nucleus and pp, while the uncertainties on signal extraction and Monte-Carlo input are considered as uncorrelated. The 8% uncertainty related to the \sqrt{s} and y mismatch between the two systems is correlated as a function of p_T , while the uncertainties on the ratio in pp collisions are correlated, for each p_T bin, between forward and backward rapidity.

Finally, in Fig. 8 the p_T dependence of the $\psi(2S)$ nuclear modification factor, calculated using Eq. 2, is presented and compared with the corresponding result for J/ψ [50]. The uncertainties are obtained with the procedure used in Fig. 4, and the results are compared to the same models quoted there.

Within uncertainties, no p_T dependence of the double ratio can be seen, and consequently as a function of transverse momentum $R_{\text{pPb}}^{\psi(2S)}$ has qualitatively a similar shape as that exhibited by $R_{\text{pPb}}^{J/\psi}$, but systematically characterized by smaller values. Theoretical models, which in this case also yield the same prediction for J/ψ and $\psi(2S)$, are in fair agreement with J/ψ results, but clearly overestimate the $\psi(2S)$ nuclear modification factor values.

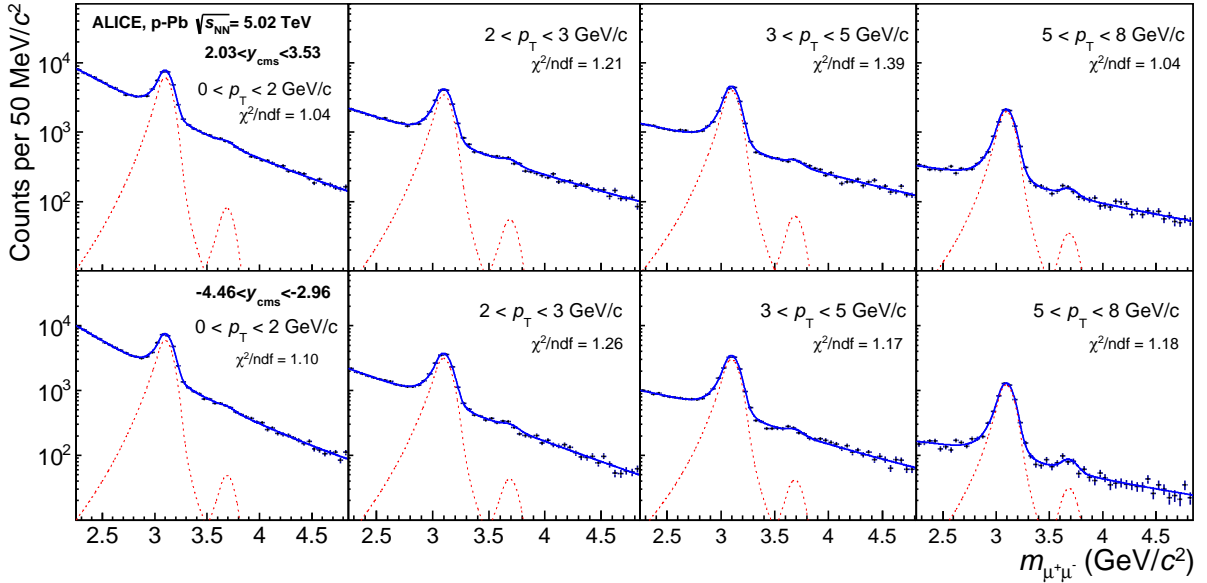


Fig. 5: Opposite-sign dimuon invariant mass spectra, in bins of transverse momentum, for the p-Pb and Pb-p data samples. For the fits shown here, Crystal Ball functions (shown as dashed lines) and a variable-width Gaussian have been used for the resonances and the background, respectively. The χ^2/ndf refers to the goodness of the signal and background combined fit in the displayed mass range.

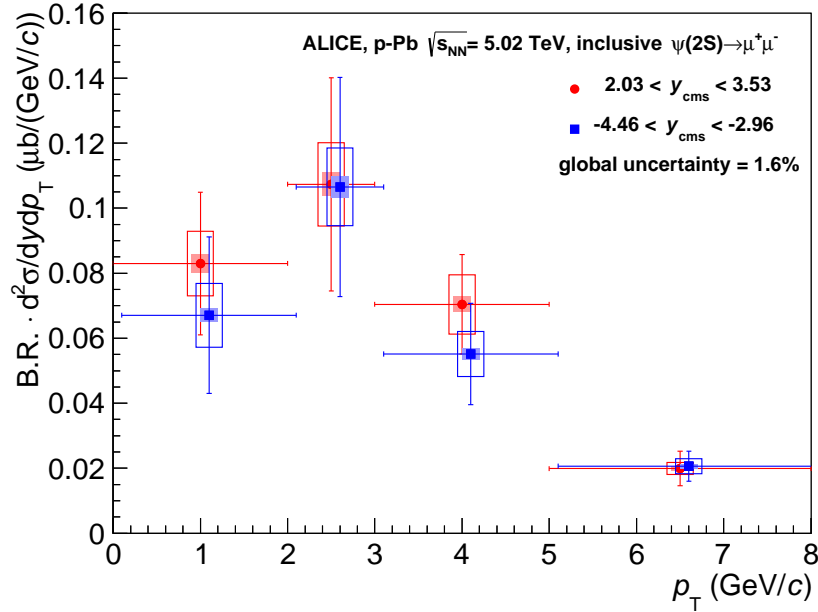


Fig. 6: The $\psi(2S)$ differential cross sections $\text{B.R.} \cdot d^2\sigma/dydp_T$ for p-Pb and Pb-p collisions. The horizontal bars correspond to the width of the transverse momentum bins. The vertical error bars correspond to the statistical uncertainties, the boxes to uncorrelated systematic uncertainties and the shaded areas to p_T -correlated uncertainties. A global 1.6% uncertainty applies to both p-Pb and Pb-p results. The points corresponding to negative y are slightly shifted in p_T to improve visibility.

It is interesting to note that different values of transverse momentum for the resonances correspond to different τ_c , with the crossing times decreasing with increasing p_T . In particular, for backward production, τ_c varies by about a factor 2, between ~ 0.07 (at $p_T = 0$) and ~ 0.03 fm/c (at $p_T = 8$ GeV/c). As a consequence, a larger fraction of $c\bar{c}$ pairs may form the final resonance state inside CNM at low p_T , and one might expect smaller values of the double ratio in that transverse momentum region due to the

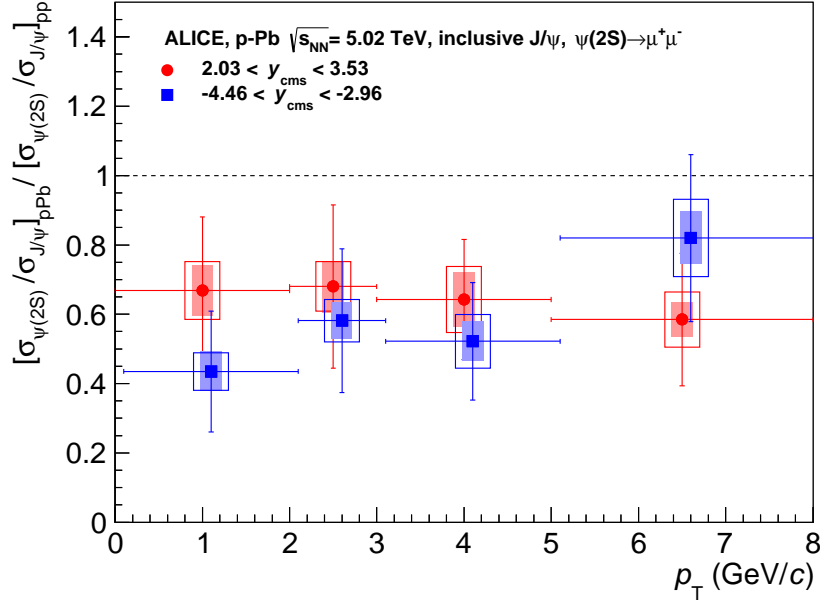


Fig. 7: The double ratio $[\sigma_{\psi(2S)}/\sigma_{J/\psi}]_{pPb}/[\sigma_{\psi(2S)}/\sigma_{J/\psi}]_{pp}$ for p-Pb and Pb-p collisions, as a function of p_T . The horizontal bars correspond to the width of the transverse momentum bins. The vertical error bars correspond to the statistical uncertainties, the boxes to uncorrelated systematic uncertainties and the shaded areas to correlated uncertainties. The points corresponding to negative y are slightly shifted in p_T to improve visibility.

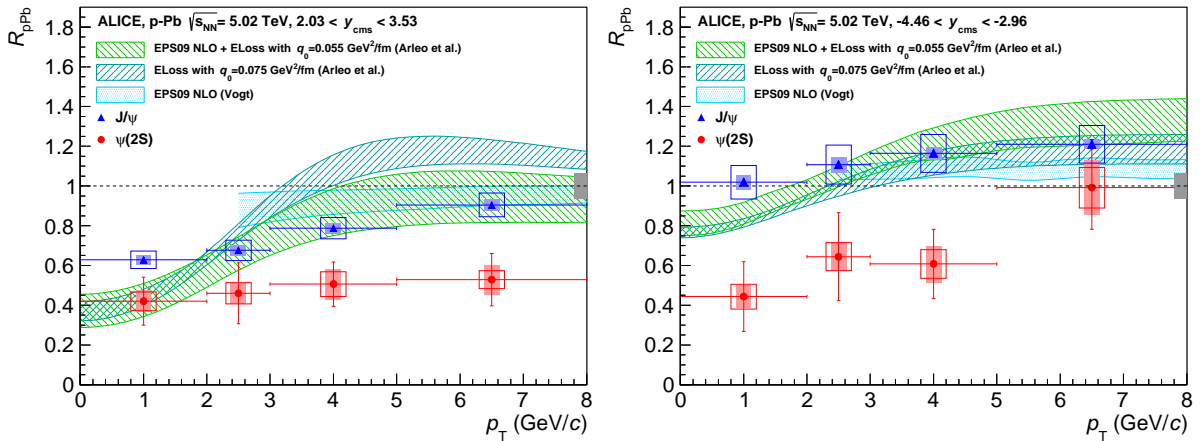


Fig. 8: The nuclear modification factor for $\psi(2S)$, compared to the corresponding quantity for J/ψ [50], as a function of p_T . Plots correspond to p-Pb (left) and Pb-p (right) collisions. The horizontal bars correspond to the width of the transverse momentum bins. The vertical error bars correspond to statistical uncertainties, the boxes to uncorrelated systematic uncertainties, and the shaded areas to partially correlated uncertainties. The filled box on the right, centered at $R_{pPb} = 1$, shows uncertainties that are fully correlated between J/ψ and $\psi(2S)$. For details on model comparisons, see the caption of Fig. 4.

weaker binding energy of $\psi(2S)$. Although the results shown in Fig. 7 could be suggestive of such a trend, no firm conclusion can be reached due to the current experimental uncertainties.

In summary, we have presented results on inclusive $\psi(2S)$ production in proton-nucleus collisions at the LHC. Measurements were performed with the ALICE Muon Spectrometer in the p-going ($2.03 < y_{cms} < 3.53$) and Pb-going ($-4.46 < y_{cms} < -2.96$) directions, and the production cross sections, the double ratios with respect to the J/ψ in p-Pb and pp and the nuclear modification factors were estimated. The results show that $\psi(2S)$ is significantly more suppressed than J/ψ in both rapidity regions, and that no p_T dependence of this effect is found within uncertainties. This observation implies that initial state nuclear effects alone cannot account for the modification of the $\psi(2S)$ yields, as also confirmed by the poor agreement of the $\psi(2S)$ R_{pPb} with models based on shadowing and/or energy loss. Final state effects, such as the pair break-up by interactions with cold nuclear matter, might in principle lead to the observed effect, but the extremely short crossing times for the $c\bar{c}$ pair, in particular at forward rapidity, make such an explanation unlikely. Consequently, other final state effects should be considered, including the interaction of the $c\bar{c}$ pair with the final state hadronic system created in the proton-nucleus collision.

Acknowledgements

The ALICE collaboration would like to thank all its engineers and technicians for their invaluable contributions to the construction of the experiment and the CERN accelerator teams for the outstanding performance of the LHC complex. The ALICE collaboration acknowledges the following funding agencies for their support in building and running the ALICE detector: State Committee of Science, World Federation of Scientists (WFS) and Swiss Fonds Kidagan, Armenia, Conselho Nacional de Desenvolvimento Científico e Tecnológico (CNPq), Financiadora de Estudos e Projetos (FINEP), Fundação de Amparo à Pesquisa do Estado de São Paulo (FAPESP); National Natural Science Foundation of China (NSFC), the Chinese Ministry of Education (CMOE) and the Ministry of Science and Technology of China (MSTC); Ministry of Education and Youth of the Czech Republic; Danish Natural Science Research Council, the Carlsberg Foundation and the Danish National Research Foundation; The European Research Council under the European Community's Seventh Framework Programme; Helsinki Institute of Physics and the Academy of Finland; French CNRS-IN2P3, the 'Region Pays de Loire', 'Region Alsace', 'Region Auvergne' and CEA, France; German BMBF and the Helmholtz Association; General Secretariat for Research and Technology, Ministry of Development, Greece; Hungarian OTKA and National Office for Research and Technology (NKTH); Department of Atomic Energy and Department of Science and Technology of the Government of India; Istituto Nazionale di Fisica Nucleare (INFN) and Centro Fermi - Museo Storico della Fisica e Centro Studi e Ricerche "Enrico Fermi", Italy; MEXT Grant-in-Aid for Specially Promoted Research, Japan; Joint Institute for Nuclear Research, Dubna; National Research Foundation of Korea (NRF); CONACYT, DGAPA, México, ALFA-EC and the EPLANET Program (European Particle Physics Latin American Network) Stichting voor Fundamenteel Onderzoek der Materie (FOM) and the Nederlandse Organisatie voor Wetenschappelijk Onderzoek (NWO), Netherlands; Research Council of Norway (NFR); Polish Ministry of Science and Higher Education; National Authority for Scientific Research - NASR (Autoritatea Națională pentru Cercetare Științifică - ANCS); Ministry of Education and Science of Russian Federation, Russian Academy of Sciences, Russian Federal Agency of Atomic Energy, Russian Federal Agency for Science and Innovations and The Russian Foundation for Basic Research; Ministry of Education of Slovakia; Department of Science and Technology, South Africa; CIEMAT, EELA, Ministerio de Economía y Competitividad (MINECO) of Spain, Xunta de Galicia (Consellería de Educación), CEADEN, Cubaenergía, Cuba, and IAEA (International Atomic Energy Agency); Swedish Research Council (VR) and Knut & Alice Wallenberg Foundation (KAW); Ukraine Ministry of Education and Science; United Kingdom Science and Technology Facilities Council (STFC); The United States Department of Energy, the United States National Science Foundation, the State of Texas, and the State of Ohio.

References

- [1] N. Brambilla et al., *Eur. Phys. J.* **C71** (2011) 1534.
- [2] G.T. Bodwin, E. Braaten and G.P. Lepage, *Phys. Rev.* **D51** (1995) 1125.
- [3] M. Butenschoen and B.A. Kniehl, *Phys. Rev. Lett.* **106** (2011) 022003.
- [4] E. Eichten et al., *Phys. Rev.* **D21** (1980) 203.
- [5] Proceedings of the QM2012 Int. Conf., *Nucl. Phys.* **A904-905** (2013).
- [6] T. Matsui and H. Satz, *Phys. Lett.* **B178** (1986) 416.
- [7] F. Karsch and H. Satz, *Z. Phys.* **C51** (1991) 209.
- [8] S. Digal, P. Petreczky and H. Satz, *Phys. Rev.* **D64** (2001) 094015.
- [9] H.-T. Ding et al., *Phys. Rev.* **D86** (2012) 014509.
- [10] P. Braun-Munzinger and J. Stachel, *Phys. Lett.* **B490** (2000) 196.
- [11] R.L. Thews, M. Schroedter and J. Rafelski, *Phys. Rev.* **C63** (2001) 054905.
- [12] A. Andronic, P. Braun-Munzinger, K. Redlich and J. Stachel, *Nucl. Phys.* **A789** (2007) 334.
- [13] J. Beringer et al. (Particle Data Group), *Phys. Rev.* **D86** (2012) 010001.
- [14] B. Alessandro et al. (NA50 Collaboration), *Eur. Phys. J.* **C39** (2005) 335.
- [15] B. Alessandro et al. (NA50 Collaboration), *Eur. Phys. J.* **C49** (2007) 559.
- [16] B. Alessandro et al. (NA50 Collaboration), *Eur. Phys. J.* **C48** (2006) 329.
- [17] M.J. Leitch et al. (E866 Collaboration), *Phys. Rev. Lett.* **84** (2000) 3256.
- [18] I. Abt et al. (HERA-B Collaboration), *Eur. Phys. J.* **C49** (2007) 545.
- [19] K.J. Eskola, H. Paukkunen and C.A. Salgado, *JHEP* **0904** (2009) 065.
- [20] R. Vogt, *Nucl. Phys.* **A700** (2002) 539.
- [21] B.Z. Kopeliovich and B.G. Zakharov, *Phys. Rev.* **D44** (2001) 3466.
- [22] D. McGlinchey, A.D. Frawley and R. Vogt, *Phys. Rev.* **C87** (2013) 054910.
- [23] F. Arleo and S. Peigné, *Phys. Rev. Lett.* **109** (2012) 122301.
- [24] F. Arleo, P.-B. Gossiaux, T. Gousset and J. Aichelin, *Phys. Rev.* **C61** (2000) 054906.
- [25] D. McGlinchey, A.D. Frawley and R. Vogt, *Phys. Rev.* **C87** (2013) 054910.
- [26] R. Vogt, *Phys. Rev.* **C61** (2000) 035203.
- [27] A. Adare et al. (PHENIX Collaboration), *Phys. Rev. Lett.* **111** (2013) 202301.
- [28] K. Aamodt et al. (ALICE Collaboration), *Phys. Lett.* **B704** (2011) 442.
- [29] K. Aamodt et al. (ALICE Collaboration), *JINST* **5** (2010) P03003.
- [30] E. Abbas et al. (ALICE Collaboration), *JINST* **8** (2013) P10016.
- [31] B. Abelev et al. (ALICE Collaboration), *Phys. Rev. Lett.* **109** (2012) 252302.
- [32] K. Aamodt et al. (ALICE Collaboration), *JINST* **3** (2008) S08002.
- [33] B. Abelev et al. (ALICE Collaboration), arXiv:1405.1849, accepted by JINST.
- [34] B. Abelev et al. (ALICE Collaboration), *Phys. Rev. Lett.* **110** (2013) 032301.
- [35] B. Abelev et al. (ALICE Collaboration), *JHEP* **1402** (2014) 073.
- [36] B. Abelev et al. (ALICE Collaboration), *Eur. Phys. J.* **C74** (2014) 2974.
- [37] J. Gaiser, SLAC Stanford - SLAC-255 (82.REC.JUN.83), <http://www.slac.stanford.edu/cgi-wrap/getdoc/slac-r-255.pdf>, page 177.
- [38] R. Shahoyan, Ph.D. Thesis, Instituto Superior Técnico, Lisbon, Portugal, 2001, <http://www.cern.ch/NA50/theses/ruben.ps.gz>.
- [39] R. Aaij et al. (LHCb Collaboration), *Eur. Phys. J.* **C73** (2013) 2631.
- [40] R. Aaij et al. (LHCb Collaboration), *Eur. Phys. J.* **C72** (2013) 2100.
- [41] S. Chatrchyan et al. (CMS Collaboration), *Phys. Lett.* **B727** (2013) 381.

- [42] R. Aaij et al. (LHCb Collaboration), *Eur. Phys. J.* **C74** (2014) 2872.
- [43] T. Aaltonen et al. (CDF Collaboration), *Phys. Rev.* **D80** (2009) 031103.
- [44] A. Adare et al. (PHENIX Collaboration), *Phys. Rev. Lett.* **98** (2007) 232002.
- [45] ALICE/LHCb public note, ALICE-PUBLIC-2013-002/LHCb-CONF-2013-013.
- [46] J.L. Albacete et al., *Int. J. Mod. Phys.* **E22** (2013) 1330007 and priv. comm.
- [47] F. Arleo and S. Peigné, *JHEP* **1303** (2013) 122.
- [48] E. Ferreira et al., arXiv:1211.4749
- [49] M. Miller et al., *Ann. Rev. Nucl. Part. Sci.* **57** (2007) 205.
- [50] B. Abelev et al. (ALICE Collaboration), “Rapidity and transverse momentum dependence of the inclusive J/ψ nuclear modification factor in p-Pb collisions at $\sqrt{s_{NN}} = 5.02$ TeV”, in preparation.

A The ALICE Collaboration

B. Abelev⁶⁹, J. Adam³⁷, D. Adamová⁷⁷, M.M. Aggarwal⁸¹, M. Agnello^{105,88}, A. Agostinelli²⁶, N. Agrawal⁴⁴, Z. Ahammed¹²⁴, N. Ahmad¹⁸, I. Ahmed¹⁵, S.U. Ahn⁶², S.A. Ahn⁶², I. Aimo^{105,88}, S. Aiola¹²⁹, M. Ajaz¹⁵, A. Akindinov⁵³, S.N. Alam¹²⁴, D. Aleksandrov⁹⁴, B. Alessandro¹⁰⁵, D. Alexandre⁹⁶, A. Alici^{12,99}, A. Alkin³, J. Alme³⁵, T. Alt³⁹, S. Altinpinar¹⁷, I. Altsybeev¹²³, C. Alves Garcia Prado¹¹³, C. Andrei⁷², A. Andronic⁹¹, V. Anguelov⁸⁷, J. Anielski⁴⁹, T. Antičić⁹², F. Antinori¹⁰², P. Antonioli⁹⁹, L. Aphecetche¹⁰⁷, H. Appelshäuser⁴⁸, S. Arcelli²⁶, N. Armesto¹⁶, R. Arnaldi¹⁰⁵, T. Aronsson¹²⁹, I.C. Arsene⁹¹, M. Arslandok⁴⁸, A. Augustinus³⁴, R. Averbeck⁹¹, T.C. Awes⁷⁸, M.D. Azmi⁸³, M. Bach³⁹, A. Badalà¹⁰¹, Y.W. Baek^{40,64}, S. Bagnasco¹⁰⁵, R. Bailhache⁴⁸, R. Bala⁸⁴, A. Baldisseri¹⁴, F. Baltasar Dos Santos Pedrosa³⁴, R.C. Baral⁵⁶, R. Barbera²⁷, F. Barile³¹, G.G. Barnaföldi¹²⁸, L.S. Barnby⁹⁶, V. Barret⁶⁴, J. Bartke¹¹⁰, M. Basile²⁶, N. Bastid⁶⁴, S. Basu¹²⁴, B. Bathen⁴⁹, G. Batigne¹⁰⁷, A. Batista Camejo⁶⁴, B. Batyunya⁶¹, P.C. Batzing²¹, C. Baumann⁴⁸, I.G. Bearden⁷⁴, H. Beck⁴⁸, C. Bedda⁸⁸, N.K. Behera⁴⁴, I. Belikov⁵⁰, F. Bellini²⁶, R. Bellwied¹¹⁵, E. Belmont-Moreno⁵⁹, R. Belmont III¹²⁷, V. Belyaev⁷⁰, G. Bencedi¹²⁸, S. Beole²⁵, I. Berceau⁷², A. Bercuci⁷², Y. Berdnikov^{11,79}, D. Berenyi¹²⁸, M.E. Berger⁸⁶, R.A. Bertens⁵², D. Berzano²⁵, L. Betev³⁴, A. Bhasin⁸⁴, I.R. Bhat⁸⁴, A.K. Bhati⁸¹, B. Bhattacharjee⁴¹, J. Bhom¹²⁰, L. Bianchi²⁵, N. Bianchi⁶⁶, C. Bianchin⁵², J. Bielčák³⁷, J. Bielčíková⁷⁷, A. Bilandžić⁷⁴, S. Bjelogrić⁵², F. Blanco¹⁰, D. Blau⁹⁴, C. Blume⁴⁸, F. Bock^{68,87}, A. Bogdanov⁷⁰, H. Bøggild⁷⁴, M. Bogolyubsky¹⁰⁶, F.V. Böhmer⁸⁶, L. Boldizsár¹²⁸, M. Bombara³⁸, J. Book⁴⁸, H. Borel¹⁴, A. Borissov^{127,90}, F. Bossú⁶⁰, M. Botje⁷⁵, E. Botta²⁵, S. Böttger⁴⁷, P. Braun-Munzinger⁹¹, M. Bregant¹¹³, T. Breitner⁴⁷, T.A. Broker⁴⁸, T.A. Browning⁸⁹, M. Broz³⁷, E. Bruna¹⁰⁵, G.E. Bruno³¹, D. Budnikov⁹³, H. Buesching⁴⁸, S. Bufalino¹⁰⁵, P. Buncic³⁴, O. Busch⁸⁷, Z. Buthelezi⁶⁰, D. Caffarri²⁸, X. Cai⁷, H. Caines¹²⁹, L. Calero Diaz⁶⁶, A. Caliva⁵², E. Calvo Villar⁹⁷, P. Camerini²⁴, F. Carena³⁴, W. Carena³⁴, J. Castillo Castellanos¹⁴, E.A.R. Casula²³, V. Catanescu⁷², C. Cavicchioli³⁴, C. Ceballos Sanchez⁹, J. Cepila³⁷, P. Cerello¹⁰⁵, B. Chang¹¹⁶, S. Chapeland³⁴, J.L. Charvet¹⁴, S. Chattopadhyay¹²⁴, S. Chattopadhyay⁹⁵, V. Chelnokov³, M. Cherney⁸⁰, C. Cheshkov¹²², B. Cheynis¹²², V. Chibante Barroso³⁴, D.D. Chinellato¹¹⁵, P. Chochula³⁴, M. Chojnacki⁷⁴, S. Choudhury¹²⁴, P. Christakoglou⁷⁵, C.H. Christensen⁷⁴, P. Christiansen³², T. Chujo¹²⁰, S.U. Chung⁹⁰, C. Cicalo¹⁰⁰, L. Cifarelli^{26,12}, F. Cindolo⁹⁹, J. Cleymans⁸³, F. Colamaria³¹, D. Colella³¹, A. Collu²³, M. Colocci²⁶, G. Conesa Balbastre⁶⁵, Z. Conesa del Valle⁴⁶, M.E. Connors¹²⁹, J.G. Contreras¹¹, T.M. Cormier¹²⁷, Y. Corrales Morales²⁵, P. Cortese³⁰, I. Cortés Maldonado², M.R. Cosentino¹¹³, F. Costa³⁴, P. Crochet⁶⁴, R. Cruz Albino¹¹, E. Cuautle⁵⁸, L. Cunqueiro⁶⁶, A. Dainese¹⁰², R. Dang⁷, A. Danu⁵⁷, D. Das⁹⁵, I. Das⁴⁶, K. Das⁹⁵, S. Das⁴, A. Dash¹¹⁴, S. Dash⁴⁴, S. De¹²⁴, H. Delagrange^{1,107}, A. Deloff⁷¹, E. Dénes¹²⁸, G. D'Erasmus³¹, A. De Caro^{29,12}, G. de Cataldo⁹⁸, J. de Cuveland³⁹, A. De Falco²³, D. De Gruttola^{29,12}, N. De Marco¹⁰⁵, S. De Pasquale²⁹, R. de Rooij⁵², M.A. Diaz Corchero¹⁰, T. Dietel⁴⁹, P. Dillenseger⁴⁸, R. Divià³⁴, D. Di Bari³¹, S. Di Liberto¹⁰³, A. Di Mauro³⁴, P. Di Nezza⁶⁶, Ø. Djuvsland¹⁷, A. Dobrin⁵², T. Dobrowolski⁷¹, D. Domenicis Gimenez¹¹³, B. Dönigus⁴⁸, O. Dordic²¹, S. Dørheim⁸⁶, A.K. Dubey¹²⁴, A. Dubla⁵², L. Ducroux¹²², P. Dupieux⁶⁴, A.K. Dutta Majumdar⁹⁵, T. E. Hilden⁴², R.J. Ehlers¹²⁹, D. Elia⁹⁸, H. Engel⁴⁷, B. Erazmus^{34,107}, H.A. Erdal³⁵, D. Eschweiler³⁹, B. Espagnon⁴⁶, M. Esposito³⁴, M. Estienne¹⁰⁷, S. Esumi¹²⁰, D. Evans⁹⁶, S. Evdokimov¹⁰⁶, D. Fabris¹⁰², J. Faivre⁶⁵, D. Falchieri²⁶, A. Fantoni⁶⁶, M. Fasel⁸⁷, D. Fehlker¹⁷, L. Feldkamp⁴⁹, D. Felea⁵⁷, A. Feliciello¹⁰⁵, G. Feofilov¹²³, J. Ferencei⁷⁷, A. Fernández Téllez², E.G. Ferreira¹⁶, A. Ferretti²⁵, A. Festanti²⁸, J. Figiel¹¹⁰, M.A.S. Figueredo¹¹⁷, S. Filchagin⁹³, D. Finogeev⁵¹, F.M. Fionda³¹, E.M. Fiore³¹, E. Floratos⁸², M. Floris³⁴, S. Foertsch⁶⁰, P. Foka⁹¹, S. Fokin⁹⁴, E. Fragiaco¹⁰⁴, A. Francescon^{34,28}, U. Frankenfeld⁹¹, U. Fuchs³⁴, C. Furget⁶⁵, M. Fusco Girard²⁹, J.J. Gaardhøje⁷⁴, M. Gagliardi²⁵, A.M. Gago⁹⁷, M. Gallio²⁵, D.R. Gangadharan¹⁹, P. Ganoti⁷⁸, C. Garabatos⁹¹, E. Garcia-Solis¹³, C. Gargiulo³⁴, I. Garishvili⁶⁹, J. Gerhard³⁹, M. Germain¹⁰⁷, A. Gheata³⁴, M. Gheata^{34,57}, B. Ghidini³¹, P. Ghosh¹²⁴, S.K. Ghosh⁴, P. Gianotti⁶⁶, P. Giubellino³⁴, E. Gladysz-Dziadus¹¹⁰, P. Glässel⁸⁷, A. Gomez Ramirez⁴⁷, P. González-Zamora¹⁰, S. Gorbunov³⁹, L. Görlich¹¹⁰, S. Gotovac¹⁰⁹, L.K. Graczykowski¹²⁶, A. Grelli⁵², A. Grigoras³⁴, C. Grigoras³⁴, V. Grigoriev⁷⁰, A. Grigoryan¹, S. Grigoryan⁶¹, B. Grinyov³, N. Grion¹⁰⁴, J.F. Grosse-Oetringhaus³⁴, J.-Y. Grossiord¹²², R. Grosso³⁴, F. Guber⁵¹, R. Guernane⁶⁵, B. Guerzoni²⁶, M. Guilbaud¹²², K. Gulbrandsen⁷⁴, H. Gulkanyan¹, M. Gumbo⁸³, T. Gunji¹¹⁹, A. Gupta⁸⁴, R. Gupta⁸⁴, K. H. Khan¹⁵, R. Haake⁴⁹, Ø. Haaland¹⁷, C. Hadjidakis⁴⁶, M. Haiduc⁵⁷,

H. Hamagaki¹¹⁹, G. Hamar¹²⁸, L.D. Hanratty⁹⁶, A. Hansen⁷⁴, J.W. Harris¹²⁹, H. Hartmann³⁹, A. Harton¹³, D. Hatzifotiadou⁹⁹, S. Hayashi¹¹⁹, S.T. Heckel⁴⁸, M. Heide⁴⁹, H. Helstrup³⁵, A. Herghelegiu⁷², G. Herrera Corral¹¹, B.A. Hess³³, K.F. Hetland³⁵, B. Hippolyte⁵⁰, J. Hladky⁵⁵, P. Hristov³⁴, M. Huang¹⁷, T.J. Humanic¹⁹, N. Hussain⁴¹, D. Hutter³⁹, D.S. Hwang²⁰, R. Ilkaev⁹³, I. Ilkiv⁷¹, M. Inaba¹²⁰, G.M. Innocenti²⁵, C. Ionita³⁴, M. Ippolitov⁹⁴, M. Irfan¹⁸, M. Ivanov⁹¹, V. Ivanov⁷⁹, A. Jacholkowski²⁷, P.M. Jacobs⁶⁸, C. Jahnke¹¹³, H.J. Jang⁶², M.A. Janik¹²⁶, P.H.S.Y. Jayarathna¹¹⁵, C. Jena²⁸, S. Jena¹¹⁵, R.T. Jimenez Bustamante⁵⁸, P.G. Jones⁹⁶, H. Jung⁴⁰, A. Jusko⁹⁶, V. Kadyshchikov⁶¹, S. Kalcher³⁹, P. Kalinak⁵⁴, A. Kalweit³⁴, J. Kamin⁴⁸, J.H. Kang¹³⁰, V. Kaplin⁷⁰, S. Kar¹²⁴, A. Karasu Uysal⁶³, O. Karavichev⁵¹, T. Karavicheva⁵¹, E. Karpechev⁵¹, U. Keschull⁴⁷, R. Keidel¹³¹, D.L.D. Keijdener⁵², M. Keil SVN³⁴, M.M. Khan^{III,18}, P. Khan⁹⁵, S.A. Khan¹²⁴, A. Khanzadeev⁷⁹, Y. Kharlov¹⁰⁶, B. Kileng³⁵, B. Kim¹³⁰, D.W. Kim^{62,40}, D.J. Kim¹¹⁶, J.S. Kim⁴⁰, M. Kim⁴⁰, M. Kim¹³⁰, S. Kim²⁰, T. Kim¹³⁰, S. Kirsch³⁹, I. Kisel³⁹, S. Kiselev⁵³, A. Kisiel¹²⁶, G. Kiss¹²⁸, J.L. Klay⁶, J. Klein⁸⁷, C. Klein-Bösing⁴⁹, A. Kluge³⁴, M.L. Knichel⁹¹, A.G. Knospe¹¹¹, C. Kobdaj^{34,108}, M. Kofarago³⁴, M.K. Köhler⁹¹, T. Kollegger³⁹, A. Kolojvari¹²³, V. Kondratiev¹²³, N. Kondratyeva⁷⁰, A. Konevskikh⁵¹, V. Kovalenko¹²³, M. Kowalski¹¹⁰, S. Kox⁶⁵, G. Koyithatta Meethalevedu⁴⁴, J. Kral¹¹⁶, I. Králik⁵⁴, F. Kramer⁴⁸, A. Kravčáková³⁸, M. Krelina³⁷, M. Kretz³⁹, M. Krivda^{96,54}, F. Krizek⁷⁷, E. Kryshen³⁴, M. Krzewicki⁹¹, V. Kučera⁷⁷, Y. Kucheriaev^{I,94}, T. Kugathasan³⁴, C. Kuhn⁵⁰, P.G. Kuijjer⁷⁵, I. Kulakov⁴⁸, J. Kumar⁴⁴, P. Kurashvili⁷¹, A. Kurepin⁵¹, A.B. Kurepin⁵¹, A. Kuryakin⁹³, S. Kushpil⁷⁷, M.J. Kweon⁸⁷, Y. Kwon¹³⁰, P. Ladron de Guevara⁵⁸, C. Lagana Fernandes¹¹³, I. Lakomov⁴⁶, R. Langoy¹²⁵, C. Lara⁴⁷, A. Lardeux¹⁰⁷, A. Lattuca²⁵, S.L. La Pointe⁵², P. La Rocca²⁷, R. Lea²⁴, L. Leardini⁸⁷, G.R. Lee⁹⁶, I. Legrand³⁴, J. Lehnert⁴⁸, R.C. Lemmon⁷⁶, V. Lenti⁹⁸, E. Leogrande⁵², M. Leoncino²⁵, I. León Monzón¹¹², P. Lévai¹²⁸, S. Li^{64,7}, J. Lien¹²⁵, R. Lietava⁹⁶, S. Lindal²¹, V. Lindenstruth³⁹, C. Lippmann⁹¹, M.A. Lisa¹⁹, H.M. Ljunggren³², D.F. Lodato⁵², P.I. Loenne¹⁷, V.R. Loggins¹²⁷, V. Loginov⁷⁰, D. Lohner⁸⁷, C. Loizides⁶⁸, X. Lopez⁶⁴, E. López Torres⁹, X.-G. Lu⁸⁷, P. Luettig⁴⁸, M. Lunardon²⁸, G. Luparello⁵², R. Ma¹²⁹, A. Maevskaya⁵¹, M. Mager³⁴, D.P. Mahapatra⁵⁶, S.M. Mahmood²¹, A. Maire⁸⁷, R.D. Majka¹²⁹, M. Malaev⁷⁹, I. Maldonado Cervantes⁵⁸, L. Malinina^{IV,61}, D. Mal'Kevich⁵³, P. Malzacher⁹¹, A. Mamonov⁹³, L. Manceau¹⁰⁵, V. Manko⁹⁴, F. Manso⁶⁴, V. Manzari⁹⁸, M. Marchisone^{64,25}, J. Mares⁵⁵, G.V. Margagliotti²⁴, A. Margotti⁹⁹, A. Marín⁹¹, C. Markert¹¹¹, M. Marquard⁴⁸, I. Martashvili¹¹⁸, N.A. Martin⁹¹, P. Martinengo³⁴, M.I. Martínez², G. Martínez García¹⁰⁷, J. Martin Blanco¹⁰⁷, Y. Martynov³, A. Mas¹⁰⁷, S. Masciocchi⁹¹, M. Maserà²⁵, A. Masoni¹⁰⁰, L. Massacrier¹⁰⁷, A. Mastroserio³¹, A. Matyja¹¹⁰, C. Mayer¹¹⁰, J. Mazer¹¹⁸, M.A. Mazzoni¹⁰³, F. Meddi²², A. Menchaca-Rocha⁵⁹, J. Mercado Pérez⁸⁷, M. Meres³⁶, Y. Miake¹²⁰, K. Mikhaylov^{61,53}, L. Milano³⁴, J. Milosevic^{V,21}, A. Mischke⁵², A.N. Mishra⁴⁵, D. Miśkowiec⁹¹, J. Mitra¹²⁴, C.M. Mitu⁵⁷, J. Mlynarz¹²⁷, N. Mohammadi⁵², B. Mohanty^{73,124}, L. Molnar⁵⁰, L. Montaño Zetina¹¹, E. Montes¹⁰, M. Morando²⁸, D.A. Moreira De Godoy¹¹³, S. Moretto²⁸, A. Morsch³⁴, V. Muccifora⁶⁶, E. Mudnic¹⁰⁹, D. Mühlheim⁴⁹, S. Muhuri¹²⁴, M. Mukherjee¹²⁴, H. Müller³⁴, M.G. Munhoz¹¹³, S. Murray⁸³, L. Musa³⁴, J. Musinsky⁵⁴, B.K. Nandi⁴⁴, R. Nania⁹⁹, E. Nappi⁹⁸, C. Nattrass¹¹⁸, K. Nayak⁷³, T.K. Nayak¹²⁴, S. Nazarenko⁹³, A. Nedosekin⁵³, M. Nicassio⁹¹, M. Niculescu^{34,57}, B.S. Nielsen⁷⁴, S. Nikolaev⁹⁴, S. Nikulin⁹⁴, V. Nikulin⁷⁹, B.S. Nilsen⁸⁰, F. Noferini^{12,99}, P. Nomokonov⁶¹, G. Nooren⁵², J. Norman¹¹⁷, A. Nyanin⁹⁴, J. Nystrand¹⁷, H. Oeschler⁸⁷, S. Oh¹²⁹, S.K. Oh^{VI,40}, A. Okatan⁶³, L. Olah¹²⁸, J. Oleniacz¹²⁶, A.C. Oliveira Da Silva¹¹³, J. Onderwaater⁹¹, C. Oppedisano¹⁰⁵, A. Ortiz Velasquez³², A. Oskarsson³², J. Otwinowski⁹¹, K. Oyama⁸⁷, P. Sahoo⁴⁵, Y. Pachmayer⁸⁷, M. Pachr³⁷, P. Pagano²⁹, G. Paić⁵⁸, F. Painke³⁹, C. Pajares¹⁶, S.K. Pal¹²⁴, A. Palmeri¹⁰¹, D. Pant⁴⁴, V. Papikyan¹, G.S. Pappalardo¹⁰¹, P. Pareek⁴⁵, W.J. Park⁹¹, S. Parmar⁸¹, A. Passfeld⁴⁹, D.I. Patalakha¹⁰⁶, V. Paticchio⁹⁸, B. Paul⁹⁵, T. Pawlak¹²⁶, T. Peitzmann⁵², H. Pereira Da Costa¹⁴, E. Pereira De Oliveira Filho¹¹³, D. Peresunko⁹⁴, C.E. Pérez Lara⁷⁵, A. Pesci⁹⁹, V. Peskov⁴⁸, Y. Pestov⁵, V. Petráček³⁷, M. Petran³⁷, M. Petris⁷², M. Petrovici⁷², C. Petta²⁷, S. Piano¹⁰⁴, M. Pikna³⁶, P. Pillot¹⁰⁷, O. Pinazza^{99,34}, L. Pinsky¹¹⁵, D.B. Piyarathna¹¹⁵, M. Płoskoń⁶⁸, M. Planinic^{121,92}, J. Pluta¹²⁶, S. Pochybova¹²⁸, P.L.M. Podesta-Lerma¹¹², M.G. Poghosyan³⁴, E.H.O. Pohjoisaho⁴², B. Polichtchouk¹⁰⁶, N. Poljak⁹², A. Pop⁷², S. Porteboeuf-Houssais⁶⁴, J. Porter⁶⁸, B. Potukuchi⁸⁴, S.K. Prasad¹²⁷, R. Preghenella^{99,12}, F. Prino¹⁰⁵, C.A. Pruneau¹²⁷, I. Pshenichnov⁵¹, G. Puddu²³, P. Pujahari¹²⁷, V. Punin⁹³, J. Putschke¹²⁷, H. Qvigstad²¹, A. Rachevski¹⁰⁴, S. Raha⁴, J. Rak¹¹⁶, A. Rakotozafindrabe¹⁴, L. Ramello³⁰, R. Raniwala⁸⁵, S. Raniwala⁸⁵, S.S. Räsänen⁴², B.T. Rascanu⁴⁸, D. Rathee⁸¹, A.W. Rauf¹⁵, V. Razazi²³, K.F. Read¹¹⁸,

J.S. Real⁶⁵, K. Redlich^{VII,71}, R.J. Reed¹²⁹, A. Rehman¹⁷, P. Reichelt⁴⁸, M. Reicher⁵², F. Reidt^{87,34}, R. Renfordt⁴⁸, A.R. Reolon⁶⁶, A. Reshetin⁵¹, F. Rettig³⁹, J.-P. Revol³⁴, K. Reygers⁸⁷, V. Riabov⁷⁹, R.A. Ricci⁶⁷, T. Richert³², M. Richter²¹, P. Riedler³⁴, W. Riegler³⁴, F. Riggi²⁷, A. Rivetti¹⁰⁵, E. Rocco⁵², M. Rodríguez Cahuantzi², A. Rodriguez Manso⁷⁵, K. Røed²¹, E. Rogochaya⁶¹, S. Rohni⁸⁴, D. Rohr³⁹, D. Röhrich¹⁷, R. Romita⁷⁶, F. Ronchetti⁶⁶, L. Ronflette¹⁰⁷, P. Rosnet⁶⁴, A. Rossi³⁴, F. Roukoutakis⁸², A. Roy⁴⁵, C. Roy⁵⁰, P. Roy⁹⁵, A.J. Rubio Montero¹⁰, R. Rui²⁴, R. Russo²⁵, E. Ryabinkin⁹⁴, Y. Ryabov⁷⁹, A. Rybicki¹¹⁰, S. Sadovsky¹⁰⁶, K. Šafařík³⁴, B. Sahlmuller⁴⁸, R. Sahoo⁴⁵, P.K. Sahu⁵⁶, J. Saini¹²⁴, S. Sakai⁶⁶, C.A. Salgado¹⁶, J. Salzwedel¹⁹, S. Sambyal⁸⁴, V. Samsonov⁷⁹, X. Sanchez Castro⁵⁰, F.J. Sánchez Rodríguez¹¹², L. Šándor⁵⁴, A. Sandoval⁵⁹, M. Sano¹²⁰, G. Santagati²⁷, D. Sarkar¹²⁴, E. Scapparone⁹⁹, F. Scarlassara²⁸, R.P. Scharenberg⁸⁹, C. Schiaua⁷², R. Schicker⁸⁷, C. Schmidt⁹¹, H.R. Schmidt³³, S. Schuchmann⁴⁸, J. Schukraft³⁴, M. Schulc³⁷, T. Schuster¹²⁹, Y. Schutz^{107,34}, K. Schwarz⁹¹, K. Schweda⁹¹, G. Scioli²⁶, E. Scomparin¹⁰⁵, R. Scott¹¹⁸, G. Segato²⁸, J.E. Seger⁸⁰, Y. Sekiguchi¹¹⁹, I. Selyuzhenkov⁹¹, J. Seo⁹⁰, E. Serradilla^{10,59}, A. Sevcenco⁵⁷, A. Shabetai¹⁰⁷, G. Shabratova⁶¹, R. Shahoyan³⁴, A. Shangaraev¹⁰⁶, N. Sharma¹¹⁸, S. Sharma⁸⁴, K. Shigaki⁴³, K. Shtejer²⁵, Y. Sibiriak⁹⁴, S. Siddhanta¹⁰⁰, T. Siemiarczuk⁷¹, D. Silvermyr⁷⁸, C. Silvestre⁶⁵, G. Simatovic¹²¹, R. Singaraju¹²⁴, R. Singh⁸⁴, S. Singha^{124,73}, V. Singhal¹²⁴, B.C. Sinha¹²⁴, T. Sinha⁹⁵, B. Sitar³⁶, M. Sitta³⁰, T.B. Skaali²¹, K. Skjerdal¹⁷, M. Slupecki¹¹⁶, N. Smirnov¹²⁹, R.J.M. Snellings⁵², C. Sjøgaard³², R. Soltz⁶⁹, J. Song⁹⁰, M. Song¹³⁰, F. Soramel²⁸, S. Sorensen¹¹⁸, M. Spacek³⁷, E. Spiriti⁶⁶, I. Sputowska¹¹⁰, M. Spyropoulou-Stassinaki⁸², B.K. Srivastava⁸⁹, J. Stachel⁸⁷, I. Stan⁵⁷, G. Stefanek⁷¹, M. Steinpreis¹⁹, E. Stenlund³², G. Steyn⁶⁰, J.H. Stiller⁸⁷, D. Stocco¹⁰⁷, M. Stolpovskiy¹⁰⁶, P. Strmen³⁶, A.A.P. Suaide¹¹³, T. Sugitate⁴³, C. Suire⁴⁶, M. Suleymanov¹⁵, R. Sultanov⁵³, M. Šumbera⁷⁷, T. Susa⁹², T.J.M. Symons⁶⁸, A. Szabo³⁶, A. Szanto de Toledo¹¹³, I. Szarka³⁶, A. Szczepankiewicz³⁴, M. Szymanski¹²⁶, J. Takahashi¹¹⁴, M.A. Tangaro³¹, J.D. Tapia Takaki^{VIII,46}, A. Tarantola Peloni⁴⁸, A. Tarazona Martinez³⁴, M.G. Tarzila⁷², A. Tauro³⁴, G. Tejeda Muñoz², A. Telesca³⁴, C. Terrevoli²³, J. Thäder⁹¹, D. Thomas⁵², R. Tieulent¹²², A.R. Timmins¹¹⁵, A. Toia¹⁰², V. Trubnikov³, W.H. Trzaska¹¹⁶, T. Tsuji¹¹⁹, A. Tumkin⁹³, R. Turrisi¹⁰², T.S. Tveter²¹, K. Ullaland¹⁷, A. Uras¹²², G.L. Usai²³, M. Vajzer⁷⁷, M. Vala^{54,61}, L. Valencia Palomo⁶⁴, S. Vallero⁸⁷, P. Vande Vyvre³⁴, J. Van Der Maarel⁵², J.W. Van Hoorne³⁴, M. van Leeuwen⁵², A. Vargas², M. Vargyas¹¹⁶, R. Varma⁴⁴, M. Vasileiou⁸², A. Vasiliev⁹⁴, V. Vechernin¹²³, M. Veldhoen⁵², A. Velure¹⁷, M. Venaruzzo^{24,67}, E. Vercellin²⁵, S. Vergara Limón², R. Vernet⁸, M. Verweij¹²⁷, L. Vickovic¹⁰⁹, G. Viesti²⁸, J. Viinikainen¹¹⁶, Z. Vilakazi⁶⁰, O. Villalobos Baillie⁹⁶, A. Vinogradov⁹⁴, L. Vinogradov¹²³, Y. Vinogradov⁹³, T. Virgili²⁹, Y.P. Viyogi¹²⁴, A. Vodopyanov⁶¹, M.A. Völkl⁸⁷, K. Voloshin⁵³, S.A. Voloshin¹²⁷, G. Volpe³⁴, B. von Haller³⁴, I. Vorobyev¹²³, D. Vranic^{91,34}, J. Vrláková³⁸, B. Vulpescu⁶⁴, A. Vyushin⁹³, B. Wagner¹⁷, J. Wagner⁹¹, V. Wagner³⁷, M. Wang^{7,107}, Y. Wang⁸⁷, D. Watanabe¹²⁰, M. Weber¹¹⁵, J.P. Wessels⁴⁹, U. Westerhoff⁴⁹, J. Wiechula³³, J. Wikne²¹, M. Wilde⁴⁹, G. Wilk⁷¹, J. Wilkinson⁸⁷, M.C.S. Williams⁹⁹, B. Windelband⁸⁷, M. Winn⁸⁷, C.G. Yaldo¹²⁷, Y. Yamaguchi¹¹⁹, H. Yang⁵², P. Yang⁷, S. Yang¹⁷, S. Yano⁴³, S. Yasnopolskiy⁹⁴, J. Yi⁹⁰, Z. Yin⁷, I.-K. Yoo⁹⁰, I. Yushmanov⁹⁴, V. Zaccolo⁷⁴, C. Zach³⁷, A. Zaman¹⁵, C. Zampolli⁹⁹, S. Zaporozhets⁶¹, A. Zarochentsev¹²³, P. Závada⁵⁵, N. Zaviyalov⁹³, H. Zbroszczyk¹²⁶, I.S. Zgura⁵⁷, M. Zhalov⁷⁹, H. Zhang⁷, X. Zhang^{7,68}, Y. Zhang⁷, C. Zhao²¹, N. Zhigareva⁵³, D. Zhou⁷, F. Zhou⁷, Y. Zhou⁵², Zhou, Zhuo¹⁷, H. Zhu⁷, J. Zhu⁷, X. Zhu⁷, A. Zichichi^{12,26}, A. Zimmermann⁸⁷, M.B. Zimmermann^{49,34}, G. Zinovjev³, Y. Zoccarato¹²², M. Zyzak⁴⁸

Affiliation Notes

^I Deceased

^{II} Also at: St. Petersburg State Polytechnical University

^{III} Also at: Department of Applied Physics, Aligarh Muslim University, Aligarh, India

^{IV} Also at: M.V. Lomonosov Moscow State University, D.V. Skobeltsyn Institute of Nuclear Physics, Moscow, Russia

^V Also at: University of Belgrade, Faculty of Physics and "Vinča" Institute of Nuclear Sciences, Belgrade, Serbia

^{VI} Permanent Address: Konkuk University, Seoul, Korea

^{VII} Also at: Institute of Theoretical Physics, University of Wroclaw, Wroclaw, Poland

^{VIII} Also at: University of Kansas, Lawrence, KS, United States

Collaboration Institutes

¹ A.I. Alikhanyan National Science Laboratory (Yerevan Physics Institute) Foundation, Yerevan, Armenia

² Benemérita Universidad Autónoma de Puebla, Puebla, Mexico

³ Bogolyubov Institute for Theoretical Physics, Kiev, Ukraine

⁴ Bose Institute, Department of Physics and Centre for Astroparticle Physics and Space Science (CAPSS), Kolkata, India

⁵ Budker Institute for Nuclear Physics, Novosibirsk, Russia

⁶ California Polytechnic State University, San Luis Obispo, CA, United States

⁷ Central China Normal University, Wuhan, China

⁸ Centre de Calcul de l'IN2P3, Villeurbanne, France

⁹ Centro de Aplicaciones Tecnológicas y Desarrollo Nuclear (CEADEN), Havana, Cuba

¹⁰ Centro de Investigaciones Energéticas Medioambientales y Tecnológicas (CIEMAT), Madrid, Spain

¹¹ Centro de Investigación y de Estudios Avanzados (CINVESTAV), Mexico City and Mérida, Mexico

¹² Centro Fermi - Museo Storico della Fisica e Centro Studi e Ricerche "Enrico Fermi", Rome, Italy

¹³ Chicago State University, Chicago, USA

¹⁴ Commissariat à l'Energie Atomique, IRFU, Saclay, France

¹⁵ COMSATS Institute of Information Technology (CIIT), Islamabad, Pakistan

¹⁶ Departamento de Física de Partículas and IGFAE, Universidad de Santiago de Compostela, Santiago de Compostela, Spain

¹⁷ Department of Physics and Technology, University of Bergen, Bergen, Norway

¹⁸ Department of Physics, Aligarh Muslim University, Aligarh, India

¹⁹ Department of Physics, Ohio State University, Columbus, OH, United States

²⁰ Department of Physics, Sejong University, Seoul, South Korea

²¹ Department of Physics, University of Oslo, Oslo, Norway

²² Dipartimento di Fisica dell'Università 'La Sapienza' and Sezione INFN Rome, Italy

²³ Dipartimento di Fisica dell'Università and Sezione INFN, Cagliari, Italy

²⁴ Dipartimento di Fisica dell'Università and Sezione INFN, Trieste, Italy

²⁵ Dipartimento di Fisica dell'Università and Sezione INFN, Turin, Italy

²⁶ Dipartimento di Fisica e Astronomia dell'Università and Sezione INFN, Bologna, Italy

²⁷ Dipartimento di Fisica e Astronomia dell'Università and Sezione INFN, Catania, Italy

²⁸ Dipartimento di Fisica e Astronomia dell'Università and Sezione INFN, Padova, Italy

²⁹ Dipartimento di Fisica 'E.R. Caianiello' dell'Università and Gruppo Collegato INFN, Salerno, Italy

³⁰ Dipartimento di Scienze e Innovazione Tecnologica dell'Università del Piemonte Orientale and Gruppo Collegato INFN, Alessandria, Italy

³¹ Dipartimento Interateneo di Fisica 'M. Merlin' and Sezione INFN, Bari, Italy

³² Division of Experimental High Energy Physics, University of Lund, Lund, Sweden

³³ Eberhard Karls Universität Tübingen, Tübingen, Germany

³⁴ European Organization for Nuclear Research (CERN), Geneva, Switzerland

³⁵ Faculty of Engineering, Bergen University College, Bergen, Norway

³⁶ Faculty of Mathematics, Physics and Informatics, Comenius University, Bratislava, Slovakia

³⁷ Faculty of Nuclear Sciences and Physical Engineering, Czech Technical University in Prague, Prague, Czech Republic

³⁸ Faculty of Science, P.J. Šafárik University, Košice, Slovakia

- ³⁹ Frankfurt Institute for Advanced Studies, Johann Wolfgang Goethe-Universität Frankfurt, Frankfurt, Germany
- ⁴⁰ Gangneung-Wonju National University, Gangneung, South Korea
- ⁴¹ Gauhati University, Department of Physics, Guwahati, India
- ⁴² Helsinki Institute of Physics (HIP), Helsinki, Finland
- ⁴³ Hiroshima University, Hiroshima, Japan
- ⁴⁴ Indian Institute of Technology Bombay (IIT), Mumbai, India
- ⁴⁵ Indian Institute of Technology Indore, Indore (IITI), India
- ⁴⁶ Institut de Physique Nucléaire d'Orsay (IPNO), Université Paris-Sud, CNRS-IN2P3, Orsay, France
- ⁴⁷ Institut für Informatik, Johann Wolfgang Goethe-Universität Frankfurt, Frankfurt, Germany
- ⁴⁸ Institut für Kernphysik, Johann Wolfgang Goethe-Universität Frankfurt, Frankfurt, Germany
- ⁴⁹ Institut für Kernphysik, Westfälische Wilhelms-Universität Münster, Münster, Germany
- ⁵⁰ Institut Pluridisciplinaire Hubert Curien (IPHC), Université de Strasbourg, CNRS-IN2P3, Strasbourg, France
- ⁵¹ Institute for Nuclear Research, Academy of Sciences, Moscow, Russia
- ⁵² Institute for Subatomic Physics of Utrecht University, Utrecht, Netherlands
- ⁵³ Institute for Theoretical and Experimental Physics, Moscow, Russia
- ⁵⁴ Institute of Experimental Physics, Slovak Academy of Sciences, Košice, Slovakia
- ⁵⁵ Institute of Physics, Academy of Sciences of the Czech Republic, Prague, Czech Republic
- ⁵⁶ Institute of Physics, Bhubaneswar, India
- ⁵⁷ Institute of Space Science (ISS), Bucharest, Romania
- ⁵⁸ Instituto de Ciencias Nucleares, Universidad Nacional Autónoma de México, Mexico City, Mexico
- ⁵⁹ Instituto de Física, Universidad Nacional Autónoma de México, Mexico City, Mexico
- ⁶⁰ iThemba LABS, National Research Foundation, Somerset West, South Africa
- ⁶¹ Joint Institute for Nuclear Research (JINR), Dubna, Russia
- ⁶² Korea Institute of Science and Technology Information, Daejeon, South Korea
- ⁶³ KTO Karatay University, Konya, Turkey
- ⁶⁴ Laboratoire de Physique Corpusculaire (LPC), Clermont Université, Université Blaise Pascal, CNRS–IN2P3, Clermont-Ferrand, France
- ⁶⁵ Laboratoire de Physique Subatomique et de Cosmologie, Université Grenoble-Alpes, CNRS-IN2P3, Grenoble, France
- ⁶⁶ Laboratori Nazionali di Frascati, INFN, Frascati, Italy
- ⁶⁷ Laboratori Nazionali di Legnaro, INFN, Legnaro, Italy
- ⁶⁸ Lawrence Berkeley National Laboratory, Berkeley, CA, United States
- ⁶⁹ Lawrence Livermore National Laboratory, Livermore, CA, United States
- ⁷⁰ Moscow Engineering Physics Institute, Moscow, Russia
- ⁷¹ National Centre for Nuclear Studies, Warsaw, Poland
- ⁷² National Institute for Physics and Nuclear Engineering, Bucharest, Romania
- ⁷³ National Institute of Science Education and Research, Bhubaneswar, India
- ⁷⁴ Niels Bohr Institute, University of Copenhagen, Copenhagen, Denmark
- ⁷⁵ Nikhef, National Institute for Subatomic Physics, Amsterdam, Netherlands
- ⁷⁶ Nuclear Physics Group, STFC Daresbury Laboratory, Daresbury, United Kingdom
- ⁷⁷ Nuclear Physics Institute, Academy of Sciences of the Czech Republic, Řež u Prahy, Czech Republic
- ⁷⁸ Oak Ridge National Laboratory, Oak Ridge, TN, United States
- ⁷⁹ Petersburg Nuclear Physics Institute, Gatchina, Russia
- ⁸⁰ Physics Department, Creighton University, Omaha, NE, United States
- ⁸¹ Physics Department, Panjab University, Chandigarh, India
- ⁸² Physics Department, University of Athens, Athens, Greece
- ⁸³ Physics Department, University of Cape Town, Cape Town, South Africa
- ⁸⁴ Physics Department, University of Jammu, Jammu, India

- 85 Physics Department, University of Rajasthan, Jaipur, India
- 86 Physik Department, Technische Universität München, Munich, Germany
- 87 Physikalisches Institut, Ruprecht-Karls-Universität Heidelberg, Heidelberg, Germany
- 88 Politecnico di Torino, Turin, Italy
- 89 Purdue University, West Lafayette, IN, United States
- 90 Pusan National University, Pusan, South Korea
- 91 Research Division and ExtreMe Matter Institute EMMI, GSI Helmholtzzentrum für Schwerionenforschung, Darmstadt, Germany
- 92 Rudjer Bošković Institute, Zagreb, Croatia
- 93 Russian Federal Nuclear Center (VNIIEF), Sarov, Russia
- 94 Russian Research Centre Kurchatov Institute, Moscow, Russia
- 95 Saha Institute of Nuclear Physics, Kolkata, India
- 96 School of Physics and Astronomy, University of Birmingham, Birmingham, United Kingdom
- 97 Sección Física, Departamento de Ciencias, Pontificia Universidad Católica del Perú, Lima, Peru
- 98 Sezione INFN, Bari, Italy
- 99 Sezione INFN, Bologna, Italy
- 100 Sezione INFN, Cagliari, Italy
- 101 Sezione INFN, Catania, Italy
- 102 Sezione INFN, Padova, Italy
- 103 Sezione INFN, Rome, Italy
- 104 Sezione INFN, Trieste, Italy
- 105 Sezione INFN, Turin, Italy
- 106 SSC IHEP of NRC Kurchatov institute, Protvino, Russia
- 107 SUBATECH, Ecole des Mines de Nantes, Université de Nantes, CNRS-IN2P3, Nantes, France
- 108 Suranaree University of Technology, Nakhon Ratchasima, Thailand
- 109 Technical University of Split FESB, Split, Croatia
- 110 The Henryk Niewodniczanski Institute of Nuclear Physics, Polish Academy of Sciences, Cracow, Poland
- 111 The University of Texas at Austin, Physics Department, Austin, TX, USA
- 112 Universidad Autónoma de Sinaloa, Culiacán, Mexico
- 113 Universidade de São Paulo (USP), São Paulo, Brazil
- 114 Universidade Estadual de Campinas (UNICAMP), Campinas, Brazil
- 115 University of Houston, Houston, TX, United States
- 116 University of Jyväskylä, Jyväskylä, Finland
- 117 University of Liverpool, Liverpool, United Kingdom
- 118 University of Tennessee, Knoxville, TN, United States
- 119 University of Tokyo, Tokyo, Japan
- 120 University of Tsukuba, Tsukuba, Japan
- 121 University of Zagreb, Zagreb, Croatia
- 122 Université de Lyon, Université Lyon 1, CNRS/IN2P3, IPN-Lyon, Villeurbanne, France
- 123 V. Fock Institute for Physics, St. Petersburg State University, St. Petersburg, Russia
- 124 Variable Energy Cyclotron Centre, Kolkata, India
- 125 Vestfold University College, Tonsberg, Norway
- 126 Warsaw University of Technology, Warsaw, Poland
- 127 Wayne State University, Detroit, MI, United States
- 128 Wigner Research Centre for Physics, Hungarian Academy of Sciences, Budapest, Hungary
- 129 Yale University, New Haven, CT, United States
- 130 Yonsei University, Seoul, South Korea
- 131 Zentrum für Technologietransfer und Telekommunikation (ZTT), Fachhochschule Worms, Worms, Germany